BNL-114163-2017-JA

The ARM Cloud Radar Simulator for Global Climate Models

Bridging Field Data and Climate Models

Yuying Zhang, Shaocheng Xie, Stephen A. Klein, Roger Marchand, Pavlos Kollias, Eugene E. Clothiaux, Wuyin Lin, Karen Johnson, Dustin Swales, Alejandro Bodas-Salcedo, Shuaiqi Tang, John M. Haynes, Scott Collis, Michael Jensen, Nitin Bharadwaj, Joseph Hardin, and Bradley Isom

Clouds play an important role in Earth's radiation budget and hydrological cycle. However, current global climate models (GCMs) have difficulties in accurately simulating clouds and precipitation. To improve the representation of clouds in climate models, it is crucial to identify where simulated clouds differ from real-world observations of them. This can be difficult, since significant differences exist between how a climate model represents clouds and what instruments observe, both in terms of spatial scale and the properties of the hydrometeors that are either modeled or observed. To address these issues and minimize impacts of instrument limitations, the concept of instrument "simulators," which convert model variables into pseudoinstrument observations, has evolved with the goal to facilitate and improve the comparison of modeled clouds with observations. Many simulators have been (and continue to be) developed for a variety of instruments and purposes. A community satellite simulator package, the Cloud Feedback Model Intercomparison Project (CFMIP) Observation Simulator Package (COSP; Bodas-Salcedo et al. 2011), contains several independent satellite simulators and is being widely used in the GCM community to exploit satellite observations for model cloud evaluation (e.g., Kay et al. 2012; Klein et al. 2013; Suzuki et al. 2013; Zhang et al. 2010).

This article introduces a ground-based cloud radar simulator developed by the U.S. Department of Energy (DOE) Atmospheric Radiation Measurement (ARM) program for comparing climate model clouds with ARM observations from its vertically pointing 35-GHz radars. As compared to the radar measurements made by *CloudSat* [a satellite carrying the first spaceborne 94-GHz (3.2-mm wavelength) cloud radar], which provides near-global sampling of profiles of cloud condensate and precipitation with a vertical resolution of 500 m (Stephens et al. 2002), ARM radar measurements occur with higher temporal resolution (10 s) and finer vertical resolution (45 m). This enables users to investigate more fully the detailed vertical structures within clouds, resolve thin clouds, and quantify the diurnal variability of clouds. Particularly, ARM radars are sensitive to low-level clouds, which are difficult for the *CloudSat* radar to detect due to both surface contamination (Mace et al. 2007; Marchand et al. 2008) and a radar sensitivity of approximately −28 dBZ near the surface. Therefore, the ARM ground-based cloud observations complement measurements from space.

OVERVIEW OF THE ARM CLOUD RADAR SIMULATOR FOR GCMS. The development of the ARM cloud radar simulator has followed the COSP workflow (Fig. 1 in Bodas-Salcedo et al. 2011),

AFFILIATIONS: Zhang, Xie, Klein, and Tang—Lawrence Livermore National Laboratory, Livermore, California; Marchand—University of Washington, Seattle, Washington; Kollias—Stony Brook University, Stony Brook, New York; Clothiaux—The Pennsylvania State University, University Park, Pennsylvania; Lin, Johnson, and Jensen—Brookhaven National Laboratory, Upton, New York; Swales—CIRES and NOAA/Earth System Research Laboratory, Boulder, Colorado; Bodas-Salcedo—Met Office Hadley Centre, Exeter, United Kingdom; Haynes—Cooperative Institute for Research in the Atmosphere/Colorado State University, Fort Collins, Colorado; Collis—Argonne National Laboratory, Argonne, Illinois; Bharadwaj, Hardin, and Isom—Pacific Northwest National Laboratory, Richland, Washington
CORRESPONDING AUTHOR: Yuying Zhang, zhang24@llnl.gov

DOI:10.1175/BAMS-D-16-0258.1

©2018 American Meteorological Society
For information regarding reuse of this content and general copyright information, consult the AMS Copyright Policy.

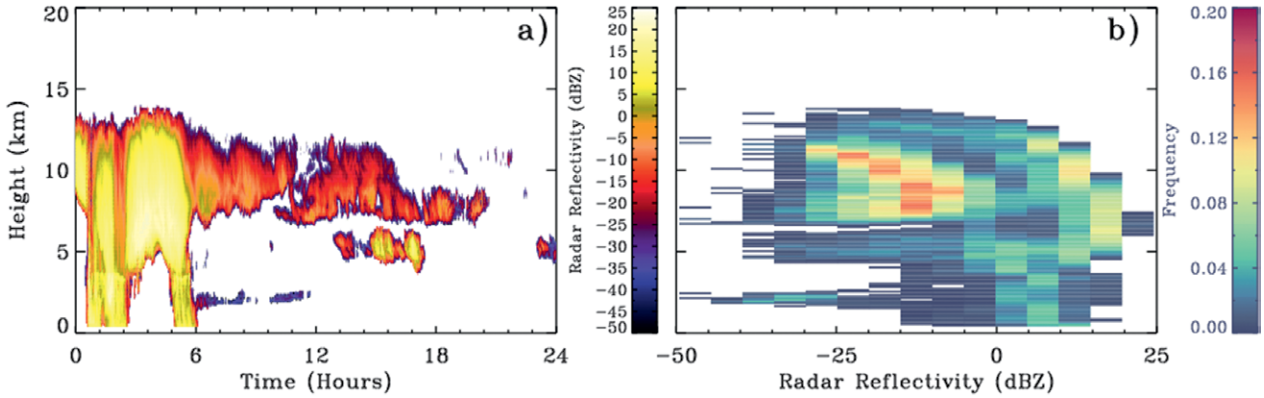

Fig. 1. Observations from the ARM SGP cloud radar on 16 May 2009. (a) Radar reflectivity from the DOE ARM ARSCL product. (b) A CFAD generated at 250-m vertical resolution from the radar reflectivities in (a).

utilizing the capabilities available in COSP wherever possible. The overarching goal of this activity is to facilitate the use of ARM detailed cloud observations by the global climate modeling community while also enhancing COSP by providing it a ground-based view of clouds. The cloud radar simulator converts model-calculated cloud properties to what a cloud radar can directly observe (i.e., radar reflectivity—a measure of the total hydrometeor backscattering cross section per unit volume). Radar reflectivity is inferred from the amount of transmitted power returned to the radar receiver after scattering from hydrometeors. The ARM cloud radar simulator is based on the QuickBeam radar simulator, implemented in COSP to calculate radar reflectivity (based on Mie theory) from input profiles of hydrometeor mixing ratios, particle sizes/types, and ambient atmospheric conditions (pressure, temperature, and relative humidity). While COSP uses QuickBeam to simulate reflectivity at 94 GHz (for comparison with *CloudSat* observations), QuickBeam is capable of simulating radar reflectivity at several microwave frequencies (Haynes et al. 2007; Marchand et al. 2009).

Adapting QuickBeam to the ARM cloud radar simulator within COSP required two changes: one was to set the frequency to 35 GHz for the ARM Ka-band cloud radar, as opposed to 94 GHz used for the *CloudSat* W-band radar, and the second was to invert the view to be from the ground to space so as to attenuate the beam correctly. In addition, the ARM cloud radar simulator uses a finer vertical resolution (100 m compared to 500 m for *CloudSat*) to resolve the more detailed structure of clouds captured by the ARM radars.

When calculating profiles of radar reflectivity based on model hydrometeor occurrence, the ARM simulator takes into consideration the minimum sensitivity of the ARM radar, as well as the saturation of the radar receiver. Simulated reflectivity values below the radar sensitivity [modeled as Eq. (1) below] are eliminated from the occurrence calculations because the ARM cloud radar would not be able to detect them, whereas values above dB*Z*_max [modeled as Eq. (2) below] are set to dB*Z*_max as it represents the saturation limiting value, which would be measured:

$$\mathrm{dBZ_min}(h) = -50 + 20 \times \log_{10} h, \qquad (1)$$

$$\mathrm{dBZ_max}(h) = 20 + 20 \times \log_{10} h, \qquad (2)$$

where h is height in kilometers. While the radar hardware and operational parameters have undergone many changes over the years, the sensitivity of the ARM radars nominally exceeds this threshold, and these same thresholds are used in the simulator and when processing the observations.

The inputs required for running the ARM cloud radar simulator are the same as those needed by the *CloudSat* simulator. These include the GCM gridbox means of the temperature and relative humidity and the hydrometeor profiles of stratiform/convective cloud fraction, cloud liquid/ice mixing ratio, precipitation fluxes with associated effective radii, and number concentrations (optional). The ARM cloud radar simulator makes use of the COSP subgrid-scale generator ("SCOPS") to produce subgrid-scale distributions of clouds and precipitation from GCM outputs to address the scale mismatch between a GCM gridbox and ARM point measurements. QuickBeam is subsequently

applied to vertical columns of the SCOPS outputs to produce a collection of subgrid-scale profiles of radar reflectivity, and the statistical module "statistical aggregation" is applied to produce statistical summaries for comparison with observations. The ARM simulator output summaries are joint histograms of radar reflectivity and altitude [i.e., the so-called Contoured Frequency by Altitude Diagrams (CFADs)].

An example of a CFAD built from observed clouds is given in Fig. 1. The occurrence of precipitating deep convective clouds between 0000 and 0600 UTC shown in Fig. 1a is reflected by the high frequencies of radar reflectivities between 15 and 25 dB*Z* at heights between 5 and 10 km and around 10 dB*Z* below 5 km in Fig. 1b. Similarly, the highest frequencies of radar reflectivity occur in bins between −25 and −5 dB*Z* at heights between 7 and 12 km; these frequencies correspond to the long-lasting anvil clouds seen after 0600 UTC in Fig. 1a.

ARM CFAD DATA. To compare with ARM cloud radar simulator outputs, observational reflectivity–height joint histograms (i.e., CFADs) are constructed from the operational ARM Active Remote Sensing of Clouds (ARSCL) Value-Added Product (Clothiaux et al. 2000). The processing starts by creating joint histograms for every hour with a 100-m vertical resolution to capture both the diurnal variability of clouds and their fine vertical structures. Similar to the *CloudSat* radar simulator, reflectivities (in dB*Z*) are binned in 5-dB*Z* increments from −50 to 25 dB*Z*. Monthly CFADs and time–height diurnal composites of hydrometeor occurrence are also produced for ease of use. To date, ARM CFADs have been generated for multiple years at five ARM sites (Table 1). In addition, ARM supports collection of radar data in other climatically significant regions through the ARM Mobile Facility (AMF) program; similar CFAD datasets will be produced from past and future AMF deployments.

For ARM Ka-band ground-based radars, insect clutter can be a big source of contamination for signals detected at lower levels, typically below 3 km. This is particularly true at the ARM Southern Great Plains (SGP) site during summertime (Luke et al. 2008). To address this issue, we produced two sets of ARM observational data based on the data quality flag "qc_ReflectivityClutterFlag" contained in the ARSCL data product. A flag value of 1 indicates that the algorithm used to produce the ARSCL data did not find evidence of clutter contaminating the hydrometeor echoes, while a flag value of 2 indicates the presence of a potential (unknown) mixture of hydrometeors and clutter. Therefore, histograms built using "qc_ReflectivityClutterFlag = 1 and 2" may overestimate cloud amount because clutter may be identified as cloud, whereas those based on "qc_ReflectivityClutterFlag = 1" may underestimate cloud amount because some hydrometeors potentially contaminated by clutter were not incorporated into the histograms. These two sets of ARM observation-based data provide estimates of upper and lower bounds on cloud occurrence by considering potential impacts of insect clutter on the data, and we are producing CFADs based on both. Figure 2 indicates that there are noticeable differences (~15%) in nonprecipitating low cloud amounts between the two data products.

APPLICATION TO GCM CLOUD EVALUATIONS. For illustration purposes, we applied the ARM radar simulator to the DOE Accelerated Climate Modeling for Energy (ACME) atmosphere model version 0. To compare with ARM data, the global ACME model was run in hindcast mode (Ma et al. 2015) with initial conditions from ERA-Interim (Dee et al. 2011). A series of 5-day hindcasts were produced every day from 0000 UTC 1 May to 0000 UTC 31 August 2009. The ARM simulator was run offline using outputs from the ACME day 2 hindcasts for this period.

Figure 3 illustrates the reflectivity–height histograms for this 4-month period produced from both the ARM observations (Fig. 3a) and ACME ARM

Table 1. ARM radar CFAD data availability.

ARM site	Lamont, Oklahoma, Southern Great Plains (SGP)	Barrow, North Slope of Alaska (NSA)	Manus Island, Tropical Western Pacific (TWPC1)	Nauru Island, Tropical Western Pacific (TWPC2)	Darwin, Australia, Tropical Western Pacific (TWPC3)
Location	36.6°N, 97.5°W	71.3°N, 156.6°W	2.0°S, 147.4°E	0.5°S, 166.9°E	12.4°S, 130.9°E
Available periods	2006–10	2012–13	2006–10	2006–08	2006–08
	2011–13		2011–13		2011–13

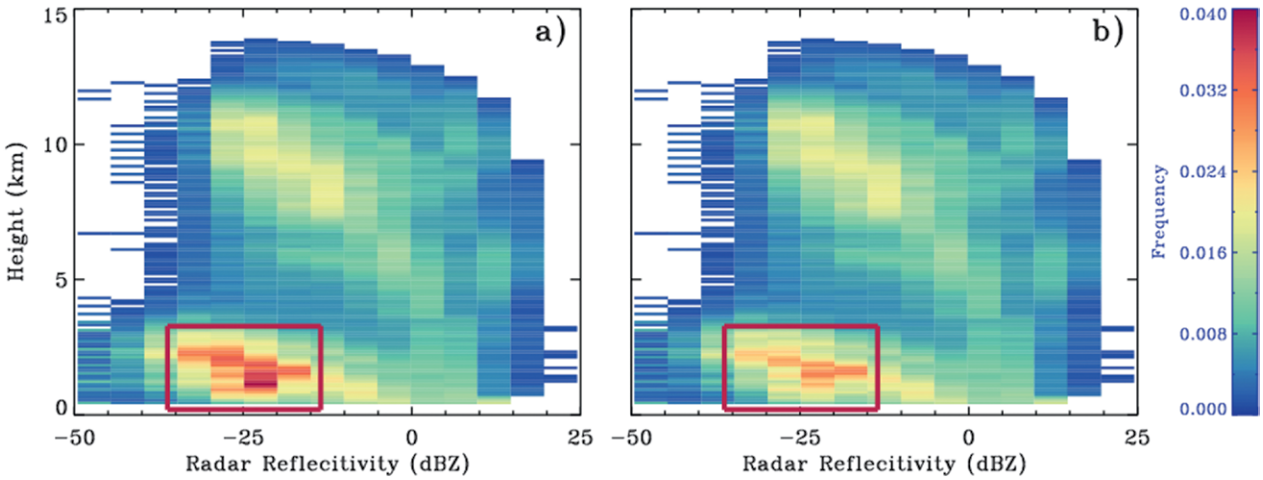

Fig. 2. Monthly-mean ARM observation-based CFADs at the ARM SGP site for May 2009. (a) qc_ReflectivityClutterFlag equal to 1 and 2, and (b) qc_ReflectivityClutterFlag equal to 1.

cloud simulator outputs (Fig. 3b). This sample comparison is for local solar time (LST) between 6:00 and 9:00 a.m. when low clouds are observed. Those clouds with a radar reflectivity less than –20 dB*Z* typically contain only small cloud droplets, and can be considered nonprecipitating. The comparison shows that the model severely underestimates the occurrence of nonprecipitating low clouds. The maximum frequency of the modeled hydrometeors between 8 and 12 km occurs in a reflectivity range of ~–15 to 0 dB*Z*, while the observed maximum occurs in the range of ~–25 to –15 dB*Z*. This indicates that the ice water content in the model is too large and/or the particle sizes are too large. The modeled occurrence of high-altitude hydrometeors is more than twice as frequent as observed, and the modeled deep clouds extend approximately 1 km deeper than those observed. Between about 2 and 7 km, the maximum frequency from the model is always above 15 dB*Z*, which is far larger than that from the observations. The lack of nonprecipitating low clouds and overestimation of high cirrus, deep convective clouds, and precipitation occurrence are common errors that exist in many state-of-the-art climate models.

As discussed earlier, one unique feature of ARM cloud radar observations with high temporal resolution is that it allows for examination of detailed cloud vertical structures over the diurnal cycle (e.g., Zhao et al. 2017). Figure 4 illustrates the observed and

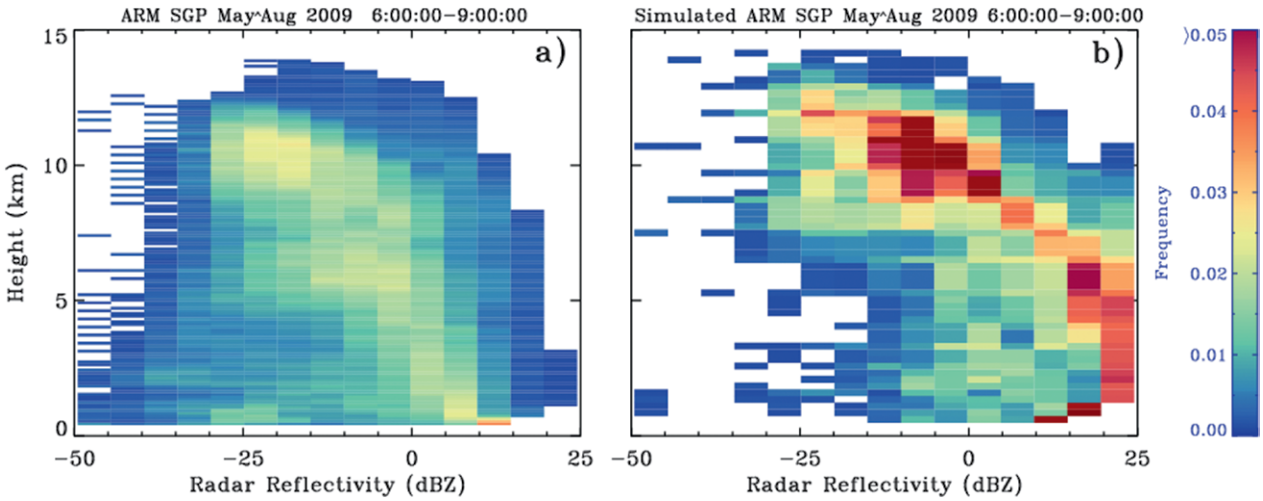

Fig. 3. CFADs for 6:00 to 9:00 a.m. LST at the ARM SGP site produced from (a) the ARM observations and (b) the ARM cloud radar simulator applied to ACME cloud outputs.

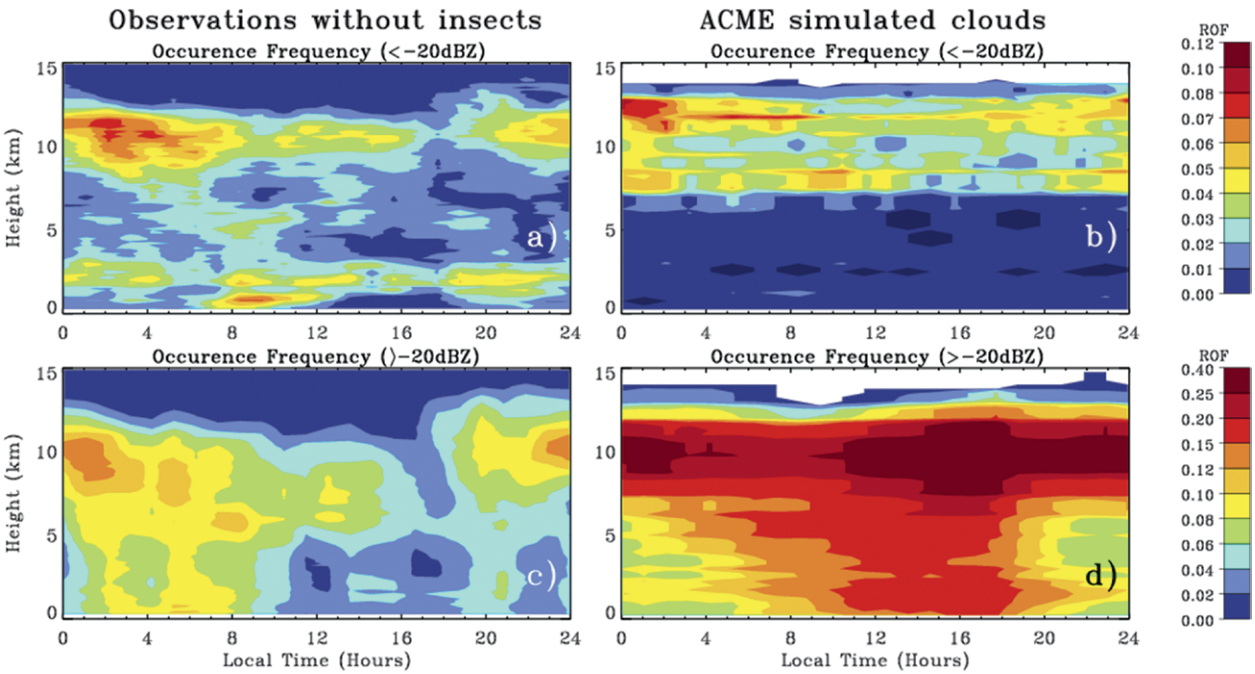

Fig. 4. (a),(c) Observed and (b),(d) modeled diurnal cycles of clouds during the summer months (i.e., May, Jun, Jul, and Aug) of 2009. (top) The relative occurrence frequencies (ROF) of nonprecipitating clouds, and (bottom) the relative occurrence frequencies of precipitating clouds.

model-based diurnal cycles of hydrometeors averaged over the 4-month period. For nonprecipitating clouds with radar reflectivities less than –20 dBZ, the model fails to capture the occurrence of shallow cumulus clouds that grow atop the daytime boundary layer (cf. Figs. 4a and 4b). For precipitating hydrometeors, estimated by the occurrence of reflectivities larger than –20 dBZ, the model significantly overestimates clouds at all levels. Finally, modeled precipitating clouds peaked in the afternoon around 4:00 p.m. LST (Fig. 4d), in contrast to the corresponding peak in the observations near midnight (Fig. 4c). The nighttime peak in observed precipitation at SGP is due largely to the impact of organized mesoscale convective systems.

SUMMARY AND FUTURE WORK. The primary purpose of developing the ARM cloud radar simulator is to facilitate the comparison of climate model–simulated clouds with ARM cloud observations such that comparisons can be done more easily and routinely, and provide insight into model performance. The ARM data are especially valuable with regard to their ability to assess model diurnal cycles of hydrometeors. It is hoped that incorporating the ARM simulator within COSP will greatly facilitate its use by the climate modeling community. This work also enhances the capability of COSP so that it can simulate cloud radar reflectivities from ground-based radars that ARM operates at its research sites. Currently, we have implemented the ARM simulator into the latest version of COSP (version 2.0) and released it as a branch in the COSP repository so that users can obtain both COSP and the ARM cloud radar simulator from one place. Both the radar simulator and CFAD data can be obtained from www.arm.gov/capabilities/vaps/radarcfad-121. Future work includes further improvements of ARM CFAD data quality via uncertainty quantification and better calibration of ARM cloud radar data. We are also considering adding diurnal cycle metrics (similar to Fig. 4) to the simulator for ease of use by the community. Zhao et al. (2017) make extensive use of this metric in evaluating the diurnal cycle of cloud and precipitation occurrence in the Multiscale Modeling Framework (MMF) climate model. They find that the MMF captures reasonably well the diurnal cycle of precipitation during the summer, but (like ACME) the MMF does not capture well the diurnal cycle of boundary layer clouds in any season.

We realize that the ARM cloud radar simulator can only provide a partial evaluation of model performance in simulating clouds given the limitations of cloud radars, such as their inability to detect small

cirrus cloud particles that leads to underestimation of cloud-top height of high thin cirrus clouds. To complement the ARM cloud radar simulator and provide a complete evaluation of model clouds, other ARM instrument simulators need to be developed, such as an ARM lidar simulator that would help identify model issues in simulating high thin cirrus clouds and a laser ceilometer simulator for providing information on cloud-base height. This additional information, along with cloud properties measured by other ARM instruments such as the Raman lidar and microwave radiometer, would help to identify other model errors.

ACKNOWLEDGMENTS. This research is supported by the U.S. DOE ARM, Atmospheric System Research, Regional and Global Climate Modeling, and Earth System Modeling programs. The authors gratefully thank the ASR/ARM Radar Science and Engineering Groups and the COSP Project Management Committee for their support and guidance. Work at LLNL was performed under the auspices of the U.S. DOE by Lawrence Livermore National Laboratory under contract DE-AC52-07NA27344. A. Bodas-Salcedo was funded by IS-ENES2 (Grant Agreement 312979). Argonne National Laboratory's work was supported by the U.S. Department of Energy, Office of Science, Office of Biological and Environmental Research, under Contract DE-AC02-06CH11357.

FOR FURTHER READING

Bodas-Salcedo, A., and Coauthors, 2011: COSP: Satellite simulation software for model assessment. *Bull. Amer. Meteor. Soc.,* **92,** 1023–1043, https://doi.org/10.1175/2011BAMS2856.1.

Clothiaux, E. E., T. P. Ackerman, G. G. Mace, K. P. Moran, R. T. Marchand, M. Miller, and B. E. Martner, 2000: Objective determination of cloud heights and radar reflectivities using a combination of active remote sensors at the ARM CART sites. *J. Appl. Meteor.,* **39,** 645–665, https://doi.org/10.1175/1520-0450(2000)039<0645:ODOCHA>2.0.CO;2.

Dee, D. P., and Coauthors, 2011: The ERA-Interim reanalysis: Configuration and performance of the data assimilation system. *Quart. J. Roy. Meteor. Soc.,* **137,** 553–597.

Haynes, J. M., R. T. Marchand, Z. Luo, A. Bodas-Salcedo, and G. L. Stephens, 2007: A multi-purpose radar simulation package: QuickBeam. *Bull. Amer. Meteor. Soc.,* **88,** 1723–1727, https://doi.org/10.1175/BAMS-88-11-1723.

Kay, J., and Coauthors, 2012: Exposing global cloud biases in the community atmosphere model (CAM) using satellite observations and their corresponding instrument simulators. *J. Climate,* **25,** 5190–5207, https://doi.org/10.1175/JCLI-D-11-00469.1.

Klein, S. A., Y. Zhang, M. D. Zelinka, R. Pincus, J. Boyle, and P. J. Gleckler, 2013: Are climate model simulations of clouds improving? An evaluation using the ISCCP simulator. *J. Geophys. Res.,* **118,** 1329–1342.

Luke, E. P., P. Kollias, K. L. Johnson, and E. E. Clothiaux, 2008: A technique for the automatic detection of insect clutter in cloud radar returns. *J. Atmos. Oceanic Technol.,* **25,** 1498–1513, https://doi.org/10.1175/2007JTECHA953.1.

Ma, H.-Y., and Coauthors, 2015: An improved hindcast approach for evaluation and diagnosis of physical processes in global climate models. *J. Adv. Model. Earth Syst.,* **7,** 1810–1827, https://doi.org/10.1002/2015MS000490.

Mace, G. G., R. Marchand, Q. Zhang, and G. Stephens, 2007: Global hydrometeor occurrence as observed by CloudSat: Initial observations from summer 2006. *Geophys. Res. Lett.,* **34,** L09808, https://doi.org/10.1029/2006GL029017.

Marchand, R., G. G. Mace, T. Ackerman, and G. Stephens, 2008: Hydrometeor detection using *CloudSat*—An Earth-orbiting 94-GHz cloud radar. *J. Atmos. Oceanic Technol.,* **25,** 519–533, https://doi.org/10.1175/2007JTECHA1006.1.

——, J. Haynes, G. G. Mace, T. Ackerman, and G. Stephens, 2009: A comparison of simulated cloud radar output from the multiscale modeling framework global climate model with CloudSat cloud radar observations. *J. Geophys. Res.,* **114,** D00A20, https://doi.org/10.1029/2008JD009790.

Stephens, G. L., and Coauthors, 2002: The *CloudSat* mission and the A-Train. *Bull. Amer. Meteor. Soc.,* **83,** 1771–1790, https://doi.org/10.1175/BAMS-83-12-1771.

Suzuki, K., J. Golaz, and G. Stephens, 2013: Evaluating cloud tuning in a climate model with satellite observations. *Geophys. Res. Lett.,* **40,** 4464–4468.

Zhang, Y., S. A. Klein, G. C. Mace, and J. Boyle, 2010: Evaluation of tropical cloud and precipitation statistics of Community Atmosphere Model version 3 using *CloudSat* and CALIPSO data. *J. Geophys. Res.,* **115,** D12205, https://doi.org/10.1029/2009JD012006.

Zhao, W., R. Marchand, and Q. Fu, 2017: The diurnal cycle of clouds and precipitation at the ARM SGP Site: Cloud radar observations and simulations from the multiscale modeling framework. *J. Geophys. Res. Atmos.,* **122,** 7519–7536.